

1 **A DISCRETE VELOCITY NUMERICAL SCHEME FOR THE 2D**
2 **BITEMPERATURE EULER SYSTEM***

3 DENISE AREGBA-DRIOLLET[†], STÉPHANE BRULL[†], AND CORENTIN. PRIGENT[‡]

4 **Abstract.** This paper is devoted to the numerical approximation of the bidimensional bitem-
5 perature Euler system. This model is a nonconservative hyperbolic system describing an out of
6 equilibrium plasma in a quasi-neutral regime, with applications in Inertial Confinement Fusion (ICF).
7 One main difficulty here is to handle shock solutions involving the product of the velocity by pressure
8 gradients. We develop a second order numerical scheme by using a discrete BGK relaxation model.
9 The second order extension is based on a subdivision of each cartesian cell into four triangles to
10 perform affine reconstructions of the solution. Such ideas have been developed in the litterature for
11 systems of conservation laws. We show here how they can be used in our nonconservative setting.
12 The numerical method is implemented and tested in the last part of the paper.

13 **Key words.** nonconservative hyperbolic system, Euler type model for plasmas, discrete BGK
14 approximation, second order

15 **AMS subject classifications.** 65M08, 35L60, 76X05, 35Q31

16 **1. Introduction.** This paper is devoted to the numerical resolution of the two
17 dimensional bitemperature Euler system by using a relaxation model under the form
18 of a discrete BGK type approximation.

19 The bitemperature Euler system is a nonconservative hyperbolic system with a
20 source term. It describes a mixture of electrons and ions in a quasi-neutral regime
21 and in a thermal nonequilibrium. This system is constituted by two conservative
22 equations for mass and momentum and two nonconservative equations on electronic
23 and ionic energies. The non-conservativity is due to source-terms but also to the
24 presence of products of the velocity by pressure gradients. Those products make
25 delicate the definition of weak solutions. Dal Maso, Le Floch and Murat developed
26 a general theory to define shocks in such a context, by using families of paths ([18]).
27 This point of view has been considered in a numerical framework ([24]). However
28 even if the path can be theoretically computed, finding the path numerically remains
29 difficult ([1]). In [17], the model is supposed to be isentropic on the electrons and
30 the system is transformed into a conservative form. The same viewpoint is adopted
31 in [20]. In [30], the authors introduce a small parameter representing the mass ratio
32 between electrons and ions. They obtain an hyperbolic system on ions and a parabolic
33 regularisation on electrons.

34 In the present paper, we generalize a discrete BGK scheme presented in [8]. In
35 this article, the bitemperature Euler system was derived as a fluid limit starting
36 from a Vlasov-BGK model coupled with Ampère and Poisson equations in a quasi-
37 neutral regime when the inter species collisions are dominant. In particular, the
38 nonconservative terms were recovered from the generalized Ohm's law giving the
39 electric field. Entropy dissipation properties were proved. Several numerical schemes
40 were proposed and compared. The approach of the present article was previously
41 validated in one space dimension and first order by comparison with the numerical
42 results of the underlying Vlasov-Maxwell system discretized at the fluid level ([8]) and

*Submitted to the editors 03/23/2021.

[†]Univ. Bordeaux, CNRS, Bordeaux INP, IMB, UMR 5251, F-33400 Talence, France
(denise.aregba@math.u-bordeaux.fr, stephane.brull@math.u-bordeaux.fr).

[‡] Univ. Bordeaux, CNRS, IMB, UMR 5251, F-33400 Talence, France (corentin.prigent@math.u-
bordeaux.fr)

43 then at the kinetic level by a DVM method ([13]). Then in [2], a Chapman-Engskog
 44 expansion was performed where diffusive terms are computed and are shown to be
 45 compatible with the entropy of the bitemperature Euler system. The resulting model
 46 is a generalization of the system considered in [15]. This underlying Vlasov-BGK
 47 model has been extended in order to take into account transverse magnetic fields in
 48 [12].

49 Discrete BGK models have been introduced in a conservative setting in [23] for
 50 the approximation of scalar conservation laws. The method was next generalized for
 51 systems in [6], (see also [7]) in the degenerate parabolic case. Entropy properties are
 52 studied in [10]. In [8], those models are generalized in order to handle the nonconser-
 53 vative terms of the 1D bitemperature Euler system. In particular, the electric force is
 54 integrated in the discrete BGK model. Those terms also make difficult the extension
 55 to second order. The ideas of [25], [26] necessitate some adaptation to preserve the
 56 properties of the first order scheme.

57 This paper is organised as follows. In section 2, the bitemperature model is
 58 introduced with the discrete BGK model that is associated. In section 3, a first order
 59 scheme is presented. It is a generalization of the numerical method of [8]. In section
 60 4, the numerical scheme is extended to second order. Finally the last part is dedicated
 61 to numerical tests.

62 2. Underlying discrete BGK model for a nonconservative Euler system.

63 **2.1. The bitemperature Euler system.** Superscripts e and i respectively de-
 64 note electronic and ionic quantities. We denote by ρ^e and ρ^i the electronic and ionic
 65 densities, $\rho = \rho^e + \rho^i$ the total density, m^e and m^i the related masses, c^e and c^i the
 66 mass fractions. These variables satisfy

$$67 \quad (2.1) \quad \rho^e = m^e n^e = c^e \rho, \quad \rho^i = m^i n^i = c^i \rho, \quad m^e > 0, \quad m^i > 0, \quad c^e + c^i = 1.$$

68 Quasineutrality is assumed, so that the ionization ratio $Z = n^e/n^i$ is a constant. This
 69 implies that the electronic and ionic mass fractions are constant and given by

$$70 \quad (2.2) \quad c^e = \frac{Zm^e}{m^i + Zm^e}, \quad c^i = \frac{m^i}{m^i + Zm^e}.$$

71 Electronic and ionic velocities u^e, u^i are assumed to be in thermodynamic equilibrium
 72 in the model. Hence, $u^e = u^i = u$, where u denotes mixture velocity. The pressure of
 73 each species satisfies a gamma-law with its own γ exponent :

$$74 \quad (2.3) \quad p^e = (\gamma^e - 1)\rho^e \varepsilon^e = n^e k_B T^e, \quad p^i = (\gamma^i - 1)\rho^i \varepsilon^i = n^i k_B T^i, \quad \gamma^e > 1, \quad \gamma^i > 1,$$

75 where k_B is the Boltzmann constant ($k_B > 0$), ε^α and T^α represent respectively the
 76 internal specific energy and the temperature of species α for $\alpha = e, i$.

77 Denoting by $|\cdot|$ the euclidean norm in \mathbb{R}^D , the total energies for the particles are
 78 defined by

$$79 \quad (2.4) \quad \mathcal{E}^\alpha = \rho^\alpha \varepsilon^\alpha + \frac{1}{2} \rho^\alpha |u|^2 = c^\alpha \left(\rho \varepsilon^\alpha + \frac{1}{2} \rho |u|^2 \right), \quad \alpha = e, i.$$

80 We denote by $\nu^{ei} \geq 0$ the interaction coefficient between the electronic and ionic tem-
 81 peratures. The model consists of two conservative equations for mass and momentum

82 and two nonconservative equations for each energy:

$$83 \quad (2.5) \quad \begin{cases} \partial_t \rho + \operatorname{div}(\rho u) = 0, \\ \partial_t(\rho u) + \operatorname{div}(\rho u \otimes u + (p^e + p^i)\mathbf{I}) = 0, \\ \partial_t \mathcal{E}^e + \operatorname{div}(u(\mathcal{E}^e + p^e)) - u \cdot \nabla (c^i p^e - c^e p^i) = \nu^{ei}(T^i - T^e), \\ \partial_t \mathcal{E}^i + \operatorname{div}(u(\mathcal{E}^i + p^i)) + u \cdot \nabla (c^i p^e - c^e p^i) = -\nu^{ei}(T^i - T^e), \end{cases}$$

84 where \mathbf{I} represents the identity matrix in \mathbb{R}^D . In the following we denote

$$85 \quad (2.6) \quad \mathcal{U} = (\rho, \rho u, \mathcal{E}^e, \mathcal{E}^i), \quad U^\alpha = (c^\alpha \rho, c^\alpha \rho u, \mathcal{E}^\alpha).$$

86 The system (2.5) is hyperbolic, diagonalisable and owns 3 eigenvalues λ_- , λ_0 (with
87 multiplicity $D + 1$ where D is the space dimension), λ_+ :

$$88 \quad \lambda_- = u \cdot \omega - a, \quad \lambda_0 = u \cdot \omega, \quad \lambda_+ = u \cdot \omega + a$$

89 where

$$90 \quad (2.7) \quad a = \sqrt{\sum_{\alpha=e,i} \frac{\gamma^\alpha p^\alpha}{\rho}}$$

91 is the sound velocity. The fields related to λ_\pm are genuinely nonlinear, while the field
92 related to λ_0 is linearly degenerate.

93 Defining the total energy $\mathcal{E} = \mathcal{E}^e + \mathcal{E}^i$ and the total pressure $p = p^e + p^i$, one
94 can note that if \mathcal{U} is a solution of system (2.5) then $(\rho, \rho u, \mathcal{E})$ satisfies the following
95 conservative system:

$$96 \quad (2.8) \quad \begin{cases} \partial_t \rho + \operatorname{div}(\rho u) = 0, \\ \partial_t(\rho u) + \operatorname{div}(\rho u \otimes u + p\mathbf{I}) = 0, \\ \partial_t \mathcal{E} + \operatorname{div}(u(\mathcal{E} + p)) = 0. \end{cases}$$

97 If $\gamma^e = \gamma^i$ this is the wellknown monotemperature Euler system. But even in this case,
98 one has to deal with one more equation to determine electronic and ionic temperatures.

99 If $\gamma^e \neq \gamma^i$ system (2.8) is not closed. We want to underline the fact that in both
100 cases, the solutions of system (2.5) are to be defined in the context of nonconservative
101 equations were the product of a possibly discontinuous function with a Dirac measure
102 appears. To give a sense to such solutions, one has to bring more physical information.
103 In [8] we obtain solutions of (2.5) as hydrodynamic limits of solutions of an underlying,
104 physically realistic BGK model. The entropy-entropy flux of species α being defined
105 as

$$106 \quad (2.9) \quad \eta^\alpha(U^\alpha) = -\frac{\rho^\alpha}{m^\alpha(\gamma^\alpha - 1)} \left[\ln \left(\frac{(\gamma^\alpha - 1)\rho^\alpha \varepsilon^\alpha}{(\rho^\alpha)^{\gamma^\alpha}} \right) + C \right], \quad Q^\alpha(U^\alpha) = \eta^\alpha(U^\alpha)u,$$

107 the total entropy-entropy flux pair for (2.5) is

$$108 \quad (2.10) \quad \eta(\mathcal{U}) = \eta^e(U^e) + \eta^i(U^i), \quad Q(\mathcal{U}) = \eta(\mathcal{U})u$$

109 and we proved the following entropy inequality for these hydrodynamic limits:

$$110 \quad (2.11) \quad \partial_t \eta(\mathcal{U}) + \operatorname{div} Q(\mathcal{U}) \leq -\frac{\nu^{ei}}{k_B T^i T^e} (T^i - T^e)^2.$$

111 We then defined an admissible solution of (2.5) as a solution satisfying this inequality.

112 We now introduce for numerical purpose a relaxing ‘‘BGK type’’ approximation
113 of system (2.5) in the spirit of [6]. It should be noted that this approximation differs
114 from the underlying BGK system mentioned just above, despite a formal resemblance.

115 **2.2. A BGK-type kinetic model for a system of conservation laws.** In
 116 order for the article to be self-contained we briefly recall the formalism for a system
 117 of conservation laws

$$118 \quad (2.12) \quad \partial_t U + \sum_{d=1}^D \partial_{x_d} F_d(U) = 0,$$

119 where $U(x, t) \in \Omega$, $\Omega \subset \mathbb{R}^K$ convex, and $F = (F_1, \dots, F_D)$ is a smooth function defined
 120 on Ω with values in $(\mathbb{R}^K)^D$. In [5], [6] we constructed relaxation approximations of
 121 such a system as a set of transport equations with source term:

$$122 \quad (2.13) \quad \partial_t f^\varepsilon + \sum_{d=1}^D \Lambda_d \partial_{x_d} f^\varepsilon = \frac{1}{\varepsilon} (M(Pf^\varepsilon) - f^\varepsilon),$$

123 with
 (2.14)

$$124 \quad f^\varepsilon = (f_1^\varepsilon, \dots, f_L^\varepsilon), \quad f^\varepsilon(x, t) \in (\mathbb{R}^K)^L, \quad \Lambda_d = \text{diag}(v_{d,1} \mathbf{I}_K, \dots, v_{d,L} \mathbf{I}_K), \quad v_{d,l} \in \mathbb{R},$$

125 $P \in \mathcal{L}((\mathbb{R}^K)^L, \mathbb{R}^K)$, and $M = (M_1, \dots, M_L)$, a function defined on Ω with values in
 126 $(\mathbb{R}^K)^L$. Equivalently we can write

$$127 \quad (2.15) \quad \partial_t f_l^\varepsilon + \sum_{d=1}^D v_{d,l} \partial_{x_d} f_l^\varepsilon = \frac{1}{\varepsilon} (M_l(Pf^\varepsilon) - f_l^\varepsilon), \quad 1 \leq l \leq L.$$

128 The compatibility between systems (2.12) and (2.13) is insured by the following con-
 129 ditions:

$$130 \quad (2.16) \quad \forall U \in \Omega, \quad P(M(U)) = U, \quad P(\Lambda_d M(U)) = F_d(U), \quad d = 1, \dots, D.$$

131 By analogy with the gas kinetic theory, we called (2.13) a discrete BGK system, M
 132 being the maxwellian function and P being the moment operator. By applying the
 133 moment operator P to (2.13) one has

$$134 \quad \partial_t (Pf^\varepsilon) + \sum_{d=1}^D \partial_{x_d} P(\Lambda_d f^\varepsilon) = 0.$$

135 Moreover, if $f^\varepsilon \rightarrow f$ then $f = M(Pf)$. Therefore, formally, $U = Pf$ is a solution of
 136 (2.12).

137 In the present article we use the following model, written for $D = 2$ for the sake
 138 of clarity. We set $L = 4$, define P as

$$139 \quad (2.17) \quad \forall f \in (\mathbb{R}^K)^4, \quad Pf = \sum_{l=1}^4 f_l.$$

140 Let $\lambda_1^+, \lambda_1^-, \lambda_2^+, \lambda_2^- \in \mathbb{R}$ be such that $\lambda_1^+ > \lambda_1^-$ and $\lambda_2^+ > \lambda_2^-$. We define the discrete
 141 velocities $V_l = (v_{1,l}, v_{2,l})$ as

$$142 \quad (2.18) \quad V_1 = (\lambda_1^-, 0), \quad V_2 = (0, \lambda_2^-), \quad V_3 = (\lambda_1^+, 0), \quad V_4 = (0, \lambda_2^+)$$

143 and the maxwellians functions

$$144 \quad (2.19) \quad M(U) = \begin{pmatrix} \frac{1}{\lambda_1^+ - \lambda_1^-} \left(\frac{\lambda_1^+}{2} U - F_1(U) \right) \\ \frac{1}{\lambda_2^+ - \lambda_2^-} \left(\frac{\lambda_2^+}{2} U - F_2(U) \right) \\ \frac{1}{\lambda_1^+ - \lambda_1^-} \left(-\frac{\lambda_1^-}{2} U + F_1(U) \right) \\ \frac{1}{\lambda_2^+ - \lambda_2^-} \left(-\frac{\lambda_2^-}{2} U + F_2(U) \right) \end{pmatrix}.$$

145 System (2.13) is a relaxation system for the “macroscopic” system (2.12), in the sense
 146 of [22], [16]. As already shown by these authors, the waves of the relaxation system
 147 (2.13) must be faster than the waves of system (2.12), that is the subcharacteristic
 148 condition. Here we need for the following condition (see [6]):

$$149 \quad (2.20) \quad \forall U \in \Omega, \quad \sigma(F'_d(U)) \subset \left] \frac{\lambda_d^-}{2}, \frac{\lambda_d^+}{2} \right[, \quad d = 1, 2$$

150 which is equivalent to

$$151 \quad (2.21) \quad \forall U \in \Omega, \quad \forall l \in \{1, \dots, L\}, \quad \sigma(M'_l(U)) \subset]0, +\infty[.$$

152 It implies entropy properties that are detailed below.

153 **2.3. BGK model for the bitemperature Euler system.** In this section, we
 154 use the model above for the development of a numerical method for the bitemper-
 155 ature Euler system, generalizing the procedure in [8]. We restrict ourselves to the
 156 bidimensional case, but the procedure is available in any space dimension.

157 **2.3.1. Construction of the model.** For $\alpha \in \{e, i\}$ we denote $F^\alpha(U^\alpha) =$
 158 $(\rho^\alpha u^\alpha, \rho^\alpha u^\alpha \otimes u^\alpha + p^\alpha \mathbf{I}, u^\alpha (\mathcal{E}^\alpha + p^\alpha))$ the flux of the conservative Euler system with
 159 the γ^α pressure law. The set of admissible states $\Omega^\alpha = \{U^\alpha \in \mathbb{R}^4, \rho^\alpha > 0, \varepsilon^\alpha > 0\}$
 160 is convex. We consider the model (2.13) with (2.14), (2.18), (2.19) for each species:
 161 we have $K = 4, L = 4$ and we denote M^α the related maxwellian function defined by
 162 (2.19). The characteristic speeds λ_d^\pm are the same for $\alpha = e$ and $\alpha = i$.

163 In order to approximate the nonconservative products, let us introduce a force
 164 term linked to the electric field $E(x, t) \in \mathbb{R}^2$:

$$165 \quad \forall \varphi = (\varphi_1, \varphi_2, \varphi_3) \in \mathbb{R} \times \mathbb{R}^2 \times \mathbb{R}, \quad N(E)\varphi = -(0, \varphi_1 E, \varphi_2 \cdot E).$$

166 For all $U^\alpha = (\rho^\alpha, \rho^\alpha u^\alpha, \mathcal{E}^\alpha) \in \mathbb{R}^4$ one has

$$167 \quad (2.22) \quad \sum_{l=1}^4 (N(E)M_l^\alpha(U^\alpha)) = N(E)U^\alpha = -(0, \rho^\alpha E, \rho^\alpha u^\alpha \cdot E).$$

168 Denoting $U^{\alpha,\varepsilon} = Pf^{\alpha,\varepsilon}$, the discrete BGK system for (2.5) is as follows ($1 \leq l \leq 4$):
 (2.23)

$$169 \quad \begin{cases} \partial_t f_l^{e,\varepsilon} + \sum_{d=1}^2 v_{d,l} \partial_{x_d} f_l^{e,\varepsilon} + \frac{q^e}{m^e} N(E^\varepsilon) f_l^{e,\varepsilon} = \frac{1}{\varepsilon} (M_l^e(U^{e,\varepsilon}) - f_l^{e,\varepsilon}) + B_l^{ei}(f^{e,\varepsilon}, f^{i,\varepsilon}), \\ \partial_t f_l^{i,\varepsilon} + \sum_{d=1}^2 v_{d,l} \partial_{x_d} f_l^{i,\varepsilon} + \frac{q^i}{m^i} N(E^\varepsilon) f_l^{i,\varepsilon} = \frac{1}{\varepsilon} (M_l^i(U^{i,\varepsilon}) - f_l^{i,\varepsilon}) + B_l^{ie}(f^{e,\varepsilon}, f^{i,\varepsilon}), \\ \partial_t E^\varepsilon = -\frac{1}{\varepsilon^2} \left(\frac{q^e}{m^e} \rho^{e,\varepsilon} u^{e,\varepsilon} + \frac{q^i}{m^i} \rho^{i,\varepsilon} u^{i,\varepsilon} \right), \\ \operatorname{div} E^\varepsilon = \frac{1}{\varepsilon^2} \left(\frac{q^e}{m^e} \rho^{e,\varepsilon} + \frac{q^i}{m^i} \rho^{i,\varepsilon} \right). \end{cases}$$

170 $q^e = -e$ and $q^i = Ze$ are respectively the electronic and ionic charges. The source
 171 terms $B^{\alpha\beta}$ model the interactions between ions and electrons, see [8]. They are such
 172 that if $\varepsilon \rightarrow 0$ then

$$173 \quad (2.24) \quad PB^{\alpha\beta} \rightarrow (0, 0, 0, \nu^{\alpha\beta}(T^\beta - T^\alpha)).$$

174 When ε tends to 0, if a limit (f^e, f^i, E) exists, then, denoting $Pf^{\alpha,\varepsilon} = U^{\alpha,\varepsilon}$ and
 175 $Pf^\alpha = U^\alpha$, we have formally:

$$176 \quad u^e = u^i = u, \quad \frac{q^e}{m^e} \rho^e + \frac{q^i}{m^i} \rho^i = 0, \quad f^\alpha = M^\alpha(U^\alpha), \quad \alpha = e, i.$$

Consequently, quasineutrality is achieved: $\rho^e = \rho c^e$ and $\rho^i = \rho c^i$ and c^e, c^i are the
 constants defined in relations (2.2). Therefore \mathcal{E}^e and \mathcal{E}^i are given by (2.4) and if
 we set $\mathcal{U} = (\rho, \rho u, \mathcal{E}^e, \mathcal{E}^i)$, then \mathcal{U}, U^e and U^i are linked by (2.6). By applying the
 moment operator P to the two first set of equations of (2.23) and taking the limit
 $\varepsilon \rightarrow 0$, it comes, for $\alpha = e, i$:

$$\begin{aligned} (2.25a) \quad & \begin{cases} \partial_t \rho^\alpha + \operatorname{div}(\rho^\alpha u) = 0, \\ \partial_t(\rho^\alpha u) + \operatorname{div}(\rho^\alpha u \otimes u) + \nabla p^\alpha - \frac{q^\alpha}{m^\alpha} E \rho^\alpha = 0, \\ \partial_t \mathcal{E}^e + \operatorname{div}(u(\mathcal{E}^e + p^e)) - q^e m^e E \rho^e u = \nu^{ei}(T^i - T^e), \\ \partial_t \mathcal{E}^i + \operatorname{div}(u(\mathcal{E}^i + p^i)) - q^i m^i E \rho^i u = -\nu^{ei}(T^i - T^e). \end{cases} \\ (2.25b) \quad & \\ (2.25c) \quad & \\ (2.25d) \quad & \end{aligned}$$

177 By taking into account the fact that c_e and c_i are constant, the first equation is just
 178 the global mass conservation, that is the first equation in (2.5). By multiplying the
 179 moment equation (2.25b) for electrons by c_i and the same equation for ions by c_e , we
 180 obtain a generalized Ohm's law for E :

$$181 \quad \frac{\rho^i q^i}{m^i} E = -\frac{\rho^e q^e}{m^e} E = -c^i \nabla p^e + c^e \nabla p^i.$$

182 Moreover, by adding equations (2.25b) for electrons and ions the force term vanishes
 183 and we obtain the second equation in (2.5). Hence $\mathcal{U} = (\rho, \rho u, \mathcal{E}^e, \mathcal{E}^i)$ is solution to
 184 the bitemperature Euler system (2.5).

185 *Remark 2.1.* The above considerations can be recast in a more general framework
 186 including continuous and discrete velocities, see [8], [4], [3] for one-dimensional cases.
 187 Here only the specific model that has been used numerically in the present article is
 188 developed.

189 **2.3.2. Solutions admissibility.** Let us now turn to the admissibility of solu-
 190 tions for the discrete velocity system (2.23). In that aim, we impose the subcharac-
 191 teristic condition (2.21) for electrons and ions, namely, using notation (2.6):

$$192 \quad (2.26) \quad \forall \mathcal{U} \in \Omega, \quad \frac{\lambda_d^-}{2} < u_d - a^\alpha < u_d + a^\alpha < \frac{\lambda_d^+}{2}, \quad \alpha = e, i, \quad d = 1, 2$$

193 where $a^\alpha = \sqrt{\frac{\gamma^\alpha p^\alpha}{\rho^\alpha}}$ is the sound velocity of each species.

194 *Remark 2.2.* The condition (2.26) does not involve the global sound speed a de-
 195 fined in (2.7). Actually $a^e \leq a$ (resp. $a^i \leq a$) if and only if $\gamma^e(\gamma^e - 1)\varepsilon^e \leq \gamma^i(\gamma^i - 1)\varepsilon^i$
 196 (resp. $\gamma^e(\gamma^e - 1)\varepsilon^e \geq \gamma^i(\gamma^i - 1)\varepsilon^i$). Hence if condition (2.26) is satisfied then one has
 197 also that

$$198 \quad \forall \mathcal{U} \in \Omega \quad \frac{\lambda_d^-}{2} < u_d - a < u_d + a < \frac{\lambda_d^+}{2}, \quad \alpha = e, i, \quad d = 1, 2.$$

199 Note that the Maxwellian functions $M_l^\alpha(U)$ can be written as linear combinations of
 200 U^α and $F^\alpha(U^\alpha)$:

$$201 \quad (2.27) \quad M_l^\alpha(U^\alpha) = \theta_l U^\alpha + \zeta_l F_1^\alpha(U^\alpha) + \chi_l F_2^\alpha(U^\alpha), \quad 1 \leq l \leq 4, \quad \alpha = e, i,$$

202 where θ_l , ζ_l and χ_l are real constants. Using the fact that $(Q_d^\alpha)'(U) = (\eta^\alpha)'(U) \circ$
 203 $(F_d^\alpha)'(U)$, it is easy to prove the following result:

204 **LEMMA 2.3.** *For $\alpha = e, i$ and $1 \leq l \leq L$ let G_l^α be the function defined by*

$$205 \quad (2.28) \quad \forall U \in \Omega^\alpha, \quad G_l^\alpha(U) = \theta_l \eta^\alpha(U) + \zeta_l Q_1^\alpha(U) + \chi_l Q_2^\alpha(U).$$

206 *Then one has*

$$207 \quad (2.29) \quad \forall U \in \Omega^\alpha, \quad (G_l^\alpha)'(U) = (\eta^\alpha)'(U) \circ (M_l^\alpha)'(U).$$

208 Our entropy result is based on the following proposition.

209 **PROPOSITION 2.4.** *([28], [10]) Let η^α , Q^α be the entropy pair defined in (2.9).
 210 Suppose that the subcharacteristic condition (2.26) is satisfied. Then M_l^α is bijective
 211 and one can define the kinetic entropies, for $1 \leq l \leq 4$ and $\alpha = e, i$:*

$$212 \quad (2.30) \quad H_l^\alpha(f_l^\alpha) = G_l^\alpha((M_l^\alpha)^{-1}(f_l^\alpha)).$$

213 *The kinetic entropies enjoy the following properties:*

- 214 • for $l = 1, \dots, 4$, the function H_l^α is convex. (E0)
- 215 • $\sum_{l=1}^4 H_l^\alpha(M_l^\alpha(U^\alpha)) = \eta^\alpha(U^\alpha)$. (E1)
- 216 • $\sum_{l=1}^4 V_l H_l^\alpha(M_l^\alpha(U^\alpha)) = Q^\alpha(U^\alpha)$. (E2)
- 217 • for all f , by denoting $U_f = P(f)$, one has $\sum_{l=1}^4 H_l^\alpha(M_l^\alpha(U_f)) \leq \sum_{l=1}^4 H_l^\alpha(f_l)$.
- 218 (E3)

219 *Such kinetic entropies are said to be entropies compatible with the macroscopic
 220 entropy η^α .*

221 Then \mathcal{U} is an admissible solution of the bitemperature Euler system, that is the
222 following theorem can be stated:

223 **THEOREM 2.5.** *Suppose that the subcharacteristic condition (2.26) is satisfied and*
224 *that $U^{\alpha,\varepsilon}, U^\alpha \in \Omega_\alpha$ for all $\varepsilon > 0$, $\alpha \in \{e, i\}$. Let \mathcal{U} be a solution of bitemperature*
225 *Euler system (2.5) obtained by passing to the limit in (2.23). Then, \mathcal{U} satisfies the*
226 *following entropy inequality:*

$$227 \quad (2.31) \quad \partial_t \eta(\mathcal{U}) + \operatorname{div} Q(\mathcal{U}) \leq -\frac{\nu^{ei}}{k_B T^i T^e} (T^i - T^e)^2.$$

228 *Proof.* First, in (2.23), take the scalar product of the equation over f_l^α by the
229 gradient $(H_l^\alpha)'(f_l^\alpha)$, and sum over l . The following equation is obtained, where $\alpha, \beta \in$
230 $\{e, i\}$ and $\alpha \neq \beta$:

$$231 \quad \partial_t \left(\sum_{l=1}^4 H_l^\alpha(f_l^{\alpha,\varepsilon}) \right) + \sum_{l=1}^4 V_l \cdot \nabla_x (H_l^\alpha(f_l^{\alpha,\varepsilon})) + \frac{q^\alpha}{m^\alpha} \sum_{l=1}^4 (H_l^\alpha)'(f_l^{\alpha,\varepsilon}) N(E) f_l^{\alpha,\varepsilon}$$

$$232 \quad = \frac{1}{\varepsilon} \sum_{l=1}^4 (H_l^\alpha)'(f_l^{\alpha,\varepsilon}) (M_l^\alpha(U^{\alpha,\varepsilon}) - f_l^{\alpha,\varepsilon}) + \sum_{l=1}^4 (H_l^\alpha)'(f_l^{\alpha,\varepsilon}) B_l^{\alpha\beta}(f_l^{\alpha,\varepsilon}, f_l^{\beta,\varepsilon}).$$

233 By convexity of H_l^α (property (E0)) and property (E3), the first term of the right-
234 hand-side satisfies the following inequality:

$$235 \quad \sum_{l=1}^4 (H_l^\alpha)'(f_l^{\alpha,\varepsilon}) (M_l^\alpha(U^{\alpha,\varepsilon}) - f_l^{\alpha,\varepsilon}) \leq \sum_{l=1}^4 (H_l^\alpha(M_l^\alpha(U^{\alpha,\varepsilon})) - H_l^\alpha(f_l^{\alpha,\varepsilon})) \leq 0.$$

237 Hence, one gets:

$$238 \quad (2.32) \quad \partial_t \left(\sum_{l=1}^4 H_l^\alpha(f_l^{\alpha,\varepsilon}) \right) + V_l \cdot \nabla_x (H_l^\alpha(f_l^{\alpha,\varepsilon})) + \frac{q^\alpha}{m^\alpha} \sum_{l=1}^4 (H_l^\alpha)'(f_l^{\alpha,\varepsilon}) N(E) f_l^{\alpha,\varepsilon}$$

$$\leq \sum_{l=1}^4 (H_l^\alpha)'(f_l^{\alpha,\varepsilon}) B_l^{\alpha\beta}(f_l^{\alpha,\varepsilon}, f_l^{\beta,\varepsilon}).$$

239 By passing formally to the limit $\varepsilon \rightarrow 0$, one has $f_l^\alpha = M_l^\alpha(U^\alpha)$ and thanks to prop-
240 erties (E1) and (E2), the inequality (2.32) becomes:

$$241 \quad (2.33) \quad \partial_t \eta^\alpha(U^\alpha) + \operatorname{div} Q^\alpha(U^\alpha) + \frac{q^\alpha}{m^\alpha} \sum_{l=1}^4 (H_l^\alpha)'(M_l^\alpha(U^\alpha)) N(E) M_l^\alpha(U^\alpha)$$

$$\leq \sum_{l=1}^4 (H_l^\alpha)'(M_l^\alpha(U^\alpha)) B_l^{\alpha\beta}(M_l^\alpha(U^\alpha), M_l^\beta(U^\beta)).$$

242 Note that applying lemma 2.3 gives

$$243 \quad (2.34) \quad \forall l \in \{1, 2, 3, 4\}, \quad (H_l^\alpha)'(M_l^\alpha(U^\alpha)) = (\eta^\alpha)'(U^\alpha)$$

244 and by a straightforward computation :

$$245 \quad (2.35) \quad (\eta^\alpha)'(U^\alpha) N(E) U^\alpha = 0.$$

246 Hence, it comes that the third term of the left-hand-side of equation (2.33) is equal
 247 to zero. Moreover, we have

$$248 \quad (2.36) \quad \frac{\partial \eta^\alpha}{\partial \mathcal{E}^\alpha}(U^\alpha) = -\frac{1}{k_B T^\alpha}$$

249 so by using again equations (2.34) and (2.24), one finds:

$$250 \quad \sum_{l=1}^4 (H_l^\alpha)'(M_l^\alpha(U^\alpha)) B_l^{\alpha\beta}(M_l^\alpha(U^\alpha), M_l^\beta(U^\beta)) = -\frac{\nu^{ei}}{k_B T^\alpha} (T^\beta - T^\alpha).$$

251 By summing over α , we obtain estimate (2.31). \square

252 3. A first order numerical scheme for the bitemperature Euler system.

253 In this section, we use the discrete BGK model presented in the previous section
 254 to design a finite volume scheme for system (2.5), following the ideas in [8]. We
 255 restrict ourselves to a cartesian grid. Denote Δx_1 and Δx_2 the space steps, Δt
 256 the time step, and $j = (j_1, j_2) \in \mathbb{Z}^2$. Denoting $e_1 = (1, 0)$, $e_2 = (0, 1)$, and for
 257 any unknown $v(x_1, x_2, t)$, v_j^n denotes its approximate value at time t^n in cell $C_j =$
 258 $]x_{1,j_1-\frac{1}{2}}, x_{1,j_1+\frac{1}{2}}[\times]x_{2,j_2-\frac{1}{2}}, x_{2,j_2+\frac{1}{2}}[$.

259 An approximate solution $(\mathcal{U}_j^n)_{j \in \mathbb{Z}^2}$ of (2.5) at time t_n being known we set

$$260 \quad (3.1) \quad U_j^{\alpha,n} = (c^\alpha \rho_j^n, c^\alpha \rho_j^n u_j^n, \mathcal{E}_j^{\alpha,n}), \quad j \in \mathbb{Z}^2 \quad \alpha = e, i.$$

261 We then approximate the discrete kinetic system (2.23).

262

263 **First step:** we set the $f_j^{\alpha,n}$ as

$$264 \quad (3.2) \quad f_j^{\alpha,n} = M^\alpha(U_j^{\alpha,n}), \quad j \in \mathbb{Z}^2, \quad \alpha = e, i.$$

265 **Second step:** we solve the linear set of transport equations $\partial_t f^\alpha + \sum_{d=1}^2 \Lambda_d \partial_{x_d} f^\alpha = 0$
 266 by the upwind scheme and apply the moment operator P . With the usual notation

$$267 \quad \forall \lambda \in \mathbb{R}, \quad \lambda^+ = \max(\lambda, 0), \quad \lambda^- = \max(-\lambda, 0), \quad \Lambda_d^\pm = \text{diag}(v_{d,l}^\pm \mathbf{I})_{1 \leq l \leq L},$$

268 we define $\forall j \in \mathbb{Z}^2$,

$$269 \quad (3.3) \quad f_j^{\alpha,n+\frac{1}{2}} = f_j^{\alpha,n} - \sum_{d=1}^2 \frac{\Delta t}{\Delta x_d} \left(h_{j+\frac{e_d}{2}}^{\alpha,n} - h_{j-\frac{e_d}{2}}^{\alpha,n} \right), \quad h_{j+\frac{e_d}{2}}^{\alpha,n} = \Lambda_d^+ f_j^{\alpha,n} - \Lambda_d^- f_{j+e_d}^{\alpha,n}.$$

270 Then we define $U_j^{\alpha,n+\frac{1}{2}}$ as $U_j^{\alpha,n+\frac{1}{2}} = P(f_j^{\alpha,n+\frac{1}{2}})$. Therefore

$$271 \quad \begin{aligned} U_j^{\alpha,n+\frac{1}{2}} &= U_j^{\alpha,n} - \sum_{d=1}^2 \frac{\Delta t}{\Delta x_d} \left(F_{j+\frac{e_d}{2}}^{\alpha,n} - F_{j-\frac{e_d}{2}}^{\alpha,n} \right), \\ F_{j+\frac{e_d}{2}}^{\alpha,n} &= \mathcal{F}_d^\alpha(U_j^{\alpha,n}, U_{j+e_d}^{\alpha,n}) \\ \mathcal{F}_d^\alpha(U, V) &= P \Lambda_d^+ M^\alpha(U) - P \Lambda_d^- M^\alpha(V) \end{aligned}$$

272 which, by the compatibility conditions (2.16), is consistent with F^α .

273 In the case of the model (2.17), (2.18), (2.19) we find

$$274 \quad (3.4) \quad \begin{cases} \text{If } 0 \leq \lambda_d^- < \lambda_d^+, & \mathcal{F}_d^\alpha(U, V) = F_d^\alpha(U), \\ \text{If } \lambda_d^- < \lambda_d^+ \leq 0, & \mathcal{F}_d^\alpha(U, V) = F_d^\alpha(V), \\ \text{If } \lambda_d^- < 0 < \lambda_d^+, & \mathcal{F}_d^\alpha(U, V) = \frac{\lambda_d^+ F_d^\alpha(U) - \lambda_d^- F_d^\alpha(V)}{\lambda_d^+ - \lambda_d^-} + \frac{\lambda_d^+ \lambda_d^- (V - U)}{2(\lambda_d^+ - \lambda_d^-)}, \end{cases}$$

275 which corresponds to the classical HLL scheme for conservation laws [29]. We recall
276 that this scheme preserves the positivity of density and temperature under appropriate
277 CFL conditions, see [19].

278 *Remark 3.1.* It is easy to see that $F_{j+\frac{e_d}{2},1}^{\alpha,n} = c^\alpha F_{j+\frac{e_d}{2},1}^n$ where $F_{j+\frac{e_d}{2},1}^n$ is as fol-
279 lows.

$$280 \quad \begin{cases} \text{If } 0 \leq \lambda_d^- < \lambda_d^+, & F_{j+\frac{e_d}{2},1}^{\alpha,n} = \rho_j^n u_{d,j}^n \\ \text{If } \lambda_d^- < \lambda_d^+ \leq 0, & F_{j+\frac{e_d}{2},1}^{\alpha,n} = \rho_{j+e_d}^n u_{d,j+e_d}^n \\ \text{If } \lambda_d^- < 0 < \lambda_d^+, & F_{j+\frac{e_d}{2},1}^{\alpha,n} = \frac{\lambda_d^+ \rho_j^n u_{d,j}^n - \lambda_d^- \rho_{j+e_d}^n u_{d,j+e_d}^n}{\lambda_d^+ - \lambda_d^-} + \frac{\lambda_d^+ \lambda_d^- (\rho_{j+e_d}^n - \rho_j^n)}{2(\lambda_d^+ - \lambda_d^-)}. \end{cases}$$

281 Hence $\rho_j^{\alpha,n+\frac{1}{2}} = c^\alpha \rho_j^{n+\frac{1}{2}}$, with

$$282 \quad (3.5) \quad \rho_j^{n+\frac{1}{2}} = \rho_j^n - \sum_{d=1}^2 \frac{\Delta t}{\Delta x_d} \left(F_{j+\frac{e_d}{2},1}^n - F_{j-\frac{e_d}{2},1}^n \right).$$

283 Our formalism allows us to prove a discrete entropy inequality. Still for model (2.17),
284 (2.18), (2.19), the upwind scheme (3.3) is monotone if and only if

$$285 \quad (3.6) \quad \forall d \in \{1, 2\}, \quad \lambda_d \frac{\Delta t}{\Delta x_d} \leq 1 \quad \text{with} \quad \lambda_d = \max(|\lambda_d^-|, |\lambda_d^+|).$$

286 If conditions (2.26) and (3.6) are satisfied then there exist discrete entropy fluxes
287 $\mathcal{G}_{j+\frac{e_d}{2},l}^{\alpha,n} = \bar{\mathcal{G}}_{d,l}^\alpha(f_{j,l}^{\alpha,n}, f_{j+e_d,l}^{\alpha,n})$ for $d = 1, 2$ such that

$$288 \quad (3.7) \quad \frac{H_l^\alpha(f_{j,l}^{\alpha,n+\frac{1}{2}}) - H_l^\alpha(f_{j,l}^{\alpha,n})}{\Delta t} + \sum_{d=1}^2 \frac{\mathcal{G}_{j+\frac{e_d}{2},l}^{\alpha,n} - \mathcal{G}_{j-\frac{e_d}{2},l}^{\alpha,n}}{\Delta x_d} \leq 0.$$

289 Namely, consistently with the exact entropy flux $V_l H_l^\alpha$:

$$290 \quad \bar{\mathcal{G}}_{d,l}^\alpha(f_{j,l}^{\alpha,n}, f_{j+e_d,l}^{\alpha,n}) = v_{d,l}^+ H_l^\alpha(f_{j,l}^{\alpha,n}) - v_{d,l}^- H_l^\alpha(f_{j+e_d,l}^{\alpha,n}), \quad d = 1, 2.$$

291 We have then

292 **LEMMA 3.2.** *We consider the model (2.17), (2.18), (2.19) and we suppose that*
293 *conditions (2.26) and (3.6) are satisfied. Then the following discrete entropy inequality*
294 *holds:*

$$295 \quad (3.8) \quad \sum_{\alpha} \frac{\eta^\alpha \left(U_j^{\alpha,n+\frac{1}{2}} \right) - \eta^\alpha \left(U_j^{\alpha,n} \right)}{\Delta t} + \sum_{d=1}^2 \frac{\mathcal{Q}_{j+\frac{e_d}{2}}^{\alpha,n} - \mathcal{Q}_{j-\frac{e_d}{2}}^{\alpha,n}}{\Delta x_d} \leq 0$$

296 where

$$297 \quad (3.9) \quad \mathcal{Q}_{j+\frac{e_d}{2}}^{\alpha,n} = \sum_{\alpha=\epsilon,i} \sum_{l=1}^4 \bar{\mathcal{G}}_{d,l}^\alpha(M_l^\alpha(U_j^{\alpha,n}), M_l^\alpha(U_{j+e_d}^{\alpha,n})) = \mathcal{Q}_d(\mathcal{U}_j^n, \mathcal{U}_{j+1}^n).$$

298 *Proof.* Sum equation (3.7) over l and over α . Thanks to properties (E3) and (E1),
 299 it comes:

$$300 \quad \sum_{l=1}^4 H_l^\alpha \left(f_{j,l}^{\alpha, n+\frac{1}{2}} \right) \geq \sum_{l=1}^4 H_l^\alpha \left(M_l^\alpha \left(\sum_{l=1}^4 f_{j,l}^{\alpha, n+\frac{1}{2}} \right) \right) = \eta^\alpha \left(\sum_{l=1}^4 f_{j,l}^{\alpha, n+\frac{1}{2}} \right),$$

301 which gives the conclusion. \square

302 **Third step:** we take into account the force terms and the source terms. For all
 303 $j \in \mathbb{Z}^2$, $\alpha, \beta \in \{e, i\}$ and $\beta \neq \alpha$, we define
 (3.10)

$$304 \quad f_{j,l}^{\alpha, n+\frac{3}{4}} = f_{j,l}^{\alpha, n+\frac{1}{2}} - \Delta t \frac{q^\alpha}{m^\alpha} N(E_j^{n+1}) f_{j,l}^{\alpha, n+1} + \Delta t B_l^{\alpha\beta} (f_j^{\alpha, n+1}, f_j^{\beta, n+1}), \quad 1 \leq l \leq 4$$

305 and

$$306 \quad (3.11) \quad U_j^{\alpha, n+1} = P(f_j^{\alpha, n+\frac{3}{4}}).$$

307 One obtains the following equations for $\alpha, \beta \in \{e, i\}$ and $\alpha \neq \beta$, $\rho_j^{n+\frac{1}{2}}$ being defined
 308 in (3.5):

$$309 \quad (3.12) \quad \rho_j^{\alpha, n+1} = c^\alpha \rho_j^{n+\frac{1}{2}}$$

310

$$311 \quad \rho_j^{\alpha, n+1} u_j^{\alpha, n+1} = \rho_j^{\alpha, n} u_j^{\alpha, n} - \sum_{d=1}^2 \frac{\Delta t}{\Delta x_d} \left(F_{j+\frac{e_d}{2}, 2}^{\alpha, n} - F_{j-\frac{e_d}{2}, 2}^{\alpha, n} \right) + \frac{\Delta t q^\alpha}{m^\alpha} E_j^{n+1} \rho_j^{\alpha, n+1}$$

312

$$313 \quad \begin{aligned} \mathcal{E}_j^{\alpha, n+1} &= \mathcal{E}_j^{\alpha, n} - \sum_{d=1}^2 \frac{\Delta t}{\Delta x_d} \left(F_{j+\frac{e_d}{2}, 3}^{\alpha, n} - F_{j-\frac{e_d}{2}, 3}^{\alpha, n} \right) \\ &+ E_j^{n+1} \cdot u_j^{n+1} \frac{\Delta t q^\alpha}{m^\alpha} \rho_j^{\alpha, n+1} + \Delta t \nu^{ei} (T_j^{\beta, n+1} - T_j^{\alpha, n+1}). \end{aligned}$$

314 Subsequently, it is necessary to ensure that the quasineutrality constraints are satis-
 315 fied, which correspond to Maxwell-Gauss and Maxwell-Ampère equations in the limit
 316 $\varepsilon \rightarrow 0$:

$$317 \quad \frac{q^e}{m^e} \rho_j^{e, n+1} + \frac{q^i}{m^i} \rho_j^{i, n+1} = 0, \quad \frac{q^e}{m^e} \rho_j^{e, n+1} u_j^{e, n+1} + \frac{q^i}{m^i} \rho_j^{i, n+1} u_j^{i, n+1} = 0.$$

318 By remark 3.1 the first condition is satisfied and $\rho_j^{n+1} = \rho_j^{e, n+1, j} + \rho_j^{i, n+1} = \rho_j^{n+\frac{1}{2}}$.

319 The second condition is equivalent to $u_j^{i, n+1} = u_j^{e, n+1} = u_j^{n+1}$. As a consequence if
 320 $U_j^{n+1} = (\rho_j^{n+1}, \rho_j^{n+1} u_j^{n+1}, \mathcal{E}_j^{e, n+1}, \mathcal{E}_j^{i, n+1})$ then $U_j^{e, n+1}$ and $U_j^{i, n+1}$ satisfy (3.1), so our
 321 notation is consistent. By applying these properties to equation (3.12) for $\alpha = e, i$,
 322 one gets:

$$323 \quad c^e \rho_j^{n+1} u_j^{n+1} = c^e \rho_j^n u_j^n - \sum_{d=1}^2 \frac{\Delta t}{\Delta x_d} \left(F_{j+\frac{e_d}{2}, 2}^{e, n} - F_{j-\frac{e_d}{2}, 2}^{e, n} \right) + \frac{\Delta t q^e}{m^e} E_j^{n+1} \rho_j^{e, n+1},$$

$$c^i \rho_j^{n+1} u_j^{n+1} = c^i \rho_j^n u_j^n - \sum_{d=1}^2 \frac{\Delta t}{\Delta x_d} \left(F_{j+\frac{e_d}{2}, 2}^{i, n} - F_{j-\frac{e_d}{2}, 2}^{i, n} \right) + \frac{\Delta t q^i}{m^i} E_j^{n+1} \rho_j^{i, n+1}.$$

324 Hence, by multiplying the first equation by c^i and the second equation by c^e , and
 325 then by subtracting one to the other, one obtains, analogously to the continuous
 326 case, the discrete generalized Ohm law:

$$327 \quad E_j^{n+1} \frac{q^i}{m^i} \rho_j^{i,n+1} = -E_j^{n+1} \frac{q^e}{m^e} \rho_j^{e,n+1} = \sum_{d=1}^2 \frac{1}{\Delta x_d} (\delta_{j+\frac{e_d}{2}}^n - \delta_{j-\frac{e_d}{2}}^n),$$

328 where nonconservative products $\delta_{j+\frac{e_d}{2}}^n$ are defined by:

$$329 \quad \delta_{j+\frac{e_d}{2}}^n = -c^i F_{j+\frac{e_d}{2},2}^{e,n} + c^e F_{j+\frac{e_d}{2},2}^{i,n} \in \mathbb{R}^2.$$

330 Remark that this approximation of nonconservative products is consistent:

$$331 \quad \delta_{j+\frac{e_d}{2}}^n = \delta_d(\mathcal{U}_j^n, \mathcal{U}_{j+e_d}^n), \quad \delta(\mathcal{U}, \mathcal{U}) = (-c^i p^e + c^e p^i) \mathbf{I}.$$

332 Finally, the numerical scheme for the total bitemperature Euler system writes:

$$(3.13) \quad \left\{ \begin{array}{l} \rho_j^{n+1} = \rho_j^n - \sum_{d=1}^2 \frac{\Delta t}{\Delta x_d} \left(F_{j+\frac{e_d}{2},1}^n - F_{j-\frac{e_d}{2},1}^n \right), \\ \rho_j^{n+1} u_j^{n+1} = \rho_j^n u_j^n - \sum_{d=1}^2 \frac{\Delta t}{\Delta x_d} \left(F_{j+\frac{e_d}{2},2}^n - F_{j-\frac{e_d}{2},2}^n \right), \\ \mathcal{E}_j^{e,n+1} = \mathcal{E}_j^{e,n} - \sum_{d=1}^2 \frac{\Delta t}{\Delta x_d} \left(F_{j+\frac{e_d}{2},3}^n - F_{j-\frac{e_d}{2},3}^n \right) \\ \quad - u_j^{n+1} \cdot \sum_{d=1}^2 \frac{\Delta t}{\Delta x_d} \left(\delta_{j+\frac{e_d}{2}}^n - \delta_{j-\frac{e_d}{2}}^n \right) + \Delta t \nu^{ei} (T_j^{i,n+1} - T_j^{e,n+1}), \\ \mathcal{E}_j^{i,n+1} = \mathcal{E}_j^{i,n} - \sum_{d=1}^2 \frac{\Delta t}{\Delta x_d} \left(F_{j+\frac{e_d}{2},4}^n - F_{j-\frac{e_d}{2},4}^n \right) \\ \quad + u_j^{n+1} \cdot \sum_{d=1}^2 \frac{\Delta t}{\Delta x_d} \left(\delta_{j+\frac{e_d}{2}}^n - \delta_{j-\frac{e_d}{2}}^n \right) - \Delta t \nu^{ei} (T_j^{i,n+1} - T_j^{e,n+1}), \end{array} \right.$$

334 with $F_{j+\frac{e_d}{2},1}^n$ defined in Remark 3.1 and

$$335 \quad F_{j+\frac{e_d}{2},2}^n = \sum_{\alpha=e,i} F_{j+\frac{e_d}{2},2}^{\alpha,n}, \quad F_{j+\frac{e_d}{2},3}^n = F_{j+\frac{e_d}{2},3}^{e,n}, \quad F_{j+\frac{e_d}{2},4}^n = F_{j+\frac{e_d}{2},4}^{i,n}.$$

336 More precisely:

$$337 \quad \delta_{j+\frac{e_d}{2}}^n = \begin{cases} \left(-c_i p_{j+e_d}^{e,n} + c_e p_{j+e_d}^{i,n} \right) e_d \text{ if } \lambda_d^- < \lambda_d^+ \leq 0, \\ \left(-c_i p_j^{e,n} + c_e p_j^{i,n} \right) e_d \text{ if } 0 \leq \lambda_d^- < \lambda_d^+, \\ \left(\frac{\lambda_d^+}{\lambda_d^+ - \lambda_d^-} (-c^i p_j^{e,n} + c^e p_j^{i,n}) - \frac{\lambda_d^-}{\lambda_d^+ - \lambda_d^-} (-c^i p_{j+e_d}^{e,n} + c^e p_{j+e_d}^{i,n}) \right) e_d \\ \quad \text{if } \lambda_d^- < 0 < \lambda_d^+. \end{cases}$$

338 Consequently, equations over partial energies can be rewritten:

$$\left\{ \begin{array}{l}
 \mathcal{E}_j^{e,n+1} = \mathcal{E}_j^{e,n} - \sum_{d=1}^2 \frac{\Delta t}{\Delta x_d} \left(F_{j+\frac{e_d}{2},3}^n - F_{j-\frac{e_d}{2},3}^n \right) \\
 \quad - \sum_{d=1}^2 u_{d,j}^{n+1} \frac{\Delta t}{\Delta x_d} \left(\delta_{j+\frac{e_d}{2},d}^n - \delta_{j-\frac{e_d}{2},d}^n \right) + \Delta t \nu^{ei} (T_j^{i,n+1} - T_j^{e,n+1}), \\
 \mathcal{E}_j^{i,n+1} = \mathcal{E}_j^{i,n} - \sum_{d=1}^2 \frac{\Delta t}{\Delta x_d} \left(F_{j+\frac{e_d}{2},4}^n - F_{j-\frac{e_d}{2},4}^n \right) \\
 \quad + \sum_{d=1}^2 u_{d,j}^{n+1} \frac{\Delta t}{\Delta x_d} \left(\delta_{j+\frac{e_d}{2},d}^n - \delta_{j-\frac{e_d}{2},d}^n \right) - \Delta t \nu^{ei} (T_j^{i,n+1} - T_j^{e,n+1}).
 \end{array} \right.$$

340 By using the following expression for temperature,

$$341 \quad T^\alpha = \frac{1}{C_v^\alpha} \left(-\frac{1}{2}|u|^2 + \frac{\mathcal{E}^\alpha}{\rho^\alpha} \right), \quad C_v^\alpha = \frac{k_B}{m^\alpha(\gamma^\alpha - 1)}, \quad \alpha \in \{e, i\},$$

342 one obtains an explicit expression of electronic and ionic energies $\mathcal{E}_j^{e,n+1}$, $\mathcal{E}_j^{i,n+1}$ as
 343 the solution of a linear 2×2 system which determinant is:

$$344 \quad 1 + \Delta t \nu^{ei} \left(\frac{1}{\rho_j^{e,n+1} C_v^e} + \frac{1}{\rho_j^{i,n+1} C_v^i} \right) \neq 0.$$

345
 346 *Remark 3.3.* By summing the expressions for $\mathcal{E}_j^{e,n+1}$ and $\mathcal{E}_j^{i,n+1}$ we observe that
 347 the approximation of $(\rho, \rho u, \mathcal{E} = \mathcal{E}^e + \mathcal{E}^i)$ is conservative, and in the case $\gamma^e = \gamma^i$ it
 348 coincides with the HLL scheme. As a consequence the positivity of ρ and of the total
 349 temperature $T = \frac{ZT^e + T^i}{Z+1}$ are preserved ([19]).

350 **THEOREM 3.4.** *We suppose that conditions (2.26) and (3.6) are satisfied. The*
 351 *numerical scheme (3.13) is entropy dissipative: with the notation (3.9)*

$$352 \quad \frac{\eta(U_j^{n+1}) - \eta(U_j^n)}{\Delta t} + \sum_{d=1}^2 \frac{Q_{j+\frac{e_d}{2}}^n - Q_{j-\frac{e_d}{2}}^n}{\Delta x_d} \leq - \frac{\nu^{ei}}{k_B T_j^{i,n+1} T_j^{e,n+1}} (T_j^{i,n+1} - T_j^{e,n+1})^2.$$

353 *Proof.* We have

$$354 \quad U_j^{\alpha,n+1} = U_j^{\alpha,n+\frac{1}{2}} - \Delta t \frac{q^\alpha}{m^\alpha} N(E_j^{n+1}) U_j^{\alpha,n+1} + \Delta t \nu^{\alpha\beta} (T_j^{\beta,n+1} - T_j^{\alpha,n+1}) e_4,$$

355 with $e_4 = (0, 0, 0, 1)$. Multiply this equation by $(\eta^\alpha)'(U_j^{\alpha,n+1})$. $(\eta^\alpha)'$ being a convex
 356 function, one gets:

$$357 \quad (3.15) \quad \eta^\alpha(U_j^{\alpha,n+1}) - \eta^\alpha(U_j^{\alpha,n+\frac{1}{2}}) \leq (\eta^\alpha)'(U_j^{\alpha,n+1}) (U_j^{\alpha,n+1} - U_j^{\alpha,n+\frac{1}{2}}).$$

358 Using properties (2.35) and (2.36) and summing equation (3.15) over α , it comes:

$$359 \quad (3.16) \quad \sum_\alpha \frac{\eta^\alpha(U_j^{\alpha,n+1}) - \eta^\alpha(U_j^{\alpha,n+\frac{1}{2}})}{\Delta t} \leq - \frac{\nu^{ei}}{k_B T_j^{i,n+1} T_j^{e,n+1}} (T_j^{i,n+1} - T_j^{e,n+1})^2.$$

360 Finally, by combining (3.8) and (3.16), and using the fact that $U_j^{e,n+1}$ and $U_j^{i,n+1}$
 361 satisfy (3.1), discrete entropy inequality (3.14) is obtained. \square

362 **4. Second-order extension.** In this section, we extend our scheme to the sec-
 363 ond order. The second order in time is reached by Heun's method. We focus our
 364 attention to second order in space. Like in [27], a piecewise affine reconstruction is
 365 used to determine intermediate values in subcells, but here this viewpoint leads to
 366 practical computations that are not required in the conservative case. Let us first
 367 recall the viewpoint for a one-dimensional system of conservation laws

$$368 \quad \partial_t U + \partial_x F(U) = 0.$$

369 Assume that a first-order conservative scheme has been chosen:

$$370 \quad U_j^{n+1} = U_j^n - \frac{\Delta t}{\Delta x} \left(F_{j+\frac{1}{2}}^n - F_{j-\frac{1}{2}}^n \right)$$

371 with $F_{j+\frac{1}{2}}^n = \mathcal{F}(U_j^n, U_{j+1}^n)$ and $\mathcal{F}(U, U) = F(U)$. Define a piecewise affine reconstruc-
 372 tion:

$$373 \quad (4.1) \quad \forall x \in C_j =]x_{j-\frac{1}{2}}, x_{j+\frac{1}{2}}[, \quad U^n(x) = U_j^n + \sigma_j^n(x - x_j), \quad x_j = \frac{1}{2}(x_{j-\frac{1}{2}} + x_{j+\frac{1}{2}}).$$

374 Once the reconstruction has been chosen, the values at the interfaces are
 (4.2)

$$375 \quad U_{j+\frac{1}{2}}^+ = (U^n(x_{j+\frac{1}{2}}))^+ = U_{j+1}^n - \sigma_{j+1}^n \frac{\Delta x}{2}, \quad U_{j+\frac{1}{2}}^- = (U^n(x_{j+\frac{1}{2}}))^- = U_j^n + \sigma_j^n \frac{\Delta x}{2}.$$

376 Then modify the first-order scheme in the following manner:

$$377 \quad (4.3) \quad U_j^{n+1} = U_j^n - \frac{\Delta t}{\Delta x} \left(\mathcal{F}(U_{j+\frac{1}{2}}^-, U_{j+\frac{1}{2}}^+) - \mathcal{F}(U_{j-\frac{1}{2}}^-, U_{j-\frac{1}{2}}^+) \right).$$

378 The stability properties of the first order scheme, such as positivity preservation, are
 379 satisfied by (4.3) under a half-CFL condition. This is due to the fact that this scheme
 380 can be interpreted as a first-order scheme defined on half-cells $C_j^- =]x_{j-\frac{1}{2}}, x_j[$ and
 381 $C_j^+ =]x_j, x_{j+\frac{1}{2}}[$, see [27] and also [11]: taking $U_{j-\frac{1}{2}}^+$ in C_j^- and $U_{j+\frac{1}{2}}^-$ in C_j^+ as initial
 382 values at time t_n , one gets:

$$383 \quad U_j^{n+1,-} = U_{j-\frac{1}{2}}^+ - \frac{2\Delta t}{\Delta x} \left(\mathcal{F}(U_{j-\frac{1}{2}}^+, U_{j+\frac{1}{2}}^-) - \mathcal{F}(U_{j-\frac{1}{2}}^-, U_{j-\frac{1}{2}}^+) \right)$$

384

$$385 \quad U_j^{n+1,+} = U_{j+\frac{1}{2}}^- - \frac{2\Delta t}{\Delta x} \left(\mathcal{F}(U_{j+\frac{1}{2}}^-, U_{j+\frac{1}{2}}^+) - \mathcal{F}(U_{j-\frac{1}{2}}^+, U_{j+\frac{1}{2}}^-) \right).$$

386 Then, the scheme (4.3) is obtained by

$$387 \quad U_j^{n+1} = \frac{1}{2} \left(U_j^{n+1,-} + U_j^{n+1,+} \right).$$

388 This procedure is extended in the case of a two-dimensional triangular mesh in [27].
 389 More developments, particularly on the limitation procedure can be found in [25], [9],
 390 [14]. It is important to note that the effective computation of the numerical fluxes at
 391 the interface of two subcells is not needed in the conservative case. It is just useful
 392 to interpretate the scheme as a combination of first order schemes. One can also
 393 add others subcells in order to realize positivity requirements, but without additional
 394 computational cost, see [9].

395 To treat the nonconservative case, we want to use the same ideas. We treat
 396 directly the case of the two-dimensional cartesian grid. Contrarily to the conserva-
 397 tive case, this algorithm necessitates the computation of the numerical fluxes at the
 398 interface of two subcells. This is a key point that leads us to detail our procedure.

399 Each cell C_j is divided into four subcells, according to figure 1.

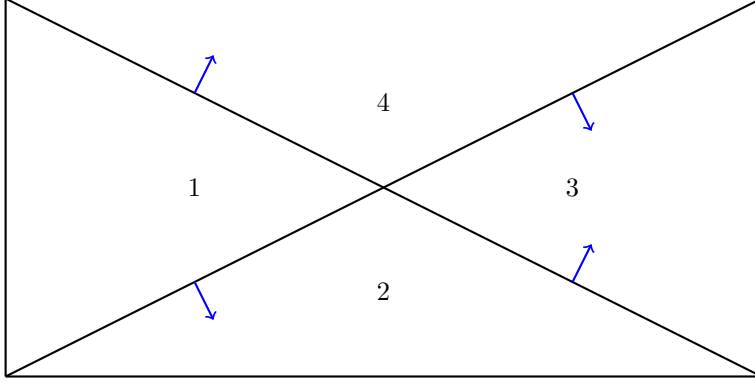


FIG. 1. For each cell C_j : subdivision into 4 triangles $T_j^{(i)}$ ($i \in \{1, 2, 3, 4\}$), and corresponding unit normal vectors.

400 Let $(\mathcal{U}_j^n)_j$ be the approximate solution at time t^n . \mathcal{U}^n is reconstructed to second-
 401 order by using slopes $\sigma_j^n = (\sigma_{1,j}^n, \sigma_{2,j}^n)$, $j \in \mathbb{Z}^2$:

$$402 \quad \forall x \in C_j, \quad \mathcal{U}(x) = \mathcal{U}_j^n + (x - x_j) \cdot \sigma_j^n.$$

403 Then, we define four constant states:

$$404 \quad \begin{aligned} \mathcal{U}_j^{(1)} &= \mathcal{U}_j^n - \frac{\Delta x_1}{2} \sigma_{1,j}^n, & \mathcal{U}_j^{(2)} &= \mathcal{U}_j^n - \frac{\Delta x_2}{2} \sigma_{2,j}^n, \\ \mathcal{U}_j^{(3)} &= \mathcal{U}_j^n + \frac{\Delta x_1}{2} \sigma_{1,j}^n, & \mathcal{U}_j^{(4)} &= \mathcal{U}_j^n + \frac{\Delta x_2}{2} \sigma_{2,j}^n. \end{aligned}$$

405 The state $\mathcal{U}_j^{(i)}$ is the initial value at time t_n in the subcell $T_j^{(i)}$ of C_j . We apply a
 406 first-order scheme to this new triangular mesh. We follow the same lines as in section
 407 3 except that we need to use the upwind scheme on triangles instead of rectangles.
 408 The positivity and entropy properties of this first order approximation are the same as
 409 as in the rectangular case.

410 We denote $T_\mu = T_j^{(i)}$, $\mathcal{U}_\mu = \mathcal{U}_j^{(i)}$. We set

$$411 \quad U_\mu^{\alpha,n} = (c^\alpha \rho_\mu^n, c^\alpha \rho_\mu^n u_\mu^n, \mathcal{E}_\mu^{\alpha,n}), \quad f_\mu^{\alpha,n} = M^\alpha(U_\mu^{\alpha,n}), \quad \alpha \in \{e, i\}.$$

412 Then we solve the linear transport set of transport equations $\partial_t f^\alpha + \sum_{d=1}^2 \Lambda_d \partial_{x_d} f^\alpha = 0$

413 by the upwind scheme. For a triangle T_μ , the adjacent triangles are denoted T_{μ_1} , T_{μ_2} ,
 414 T_{μ_3} , the outward unit normal vector from T_μ to T_{μ_k} is denoted n_k , the edge between
 415 T_μ and T_{μ_k} is denoted Γ_k . The upwind scheme then writes as
 (4.4)

$$416 \quad f_{\mu,l}^{\alpha,n+\frac{1}{2}} = f_{\mu,l}^{\alpha,n} - \frac{\Delta t}{|T_\mu|} \sum_{k=1}^3 \left((V_l \cdot n_k)^+ f_{\mu,l}^n - (V_l \cdot n_k)^- f_{\mu_k,l}^n \right) |\Gamma_k|, \quad l \in \{1, 2, 3, 4\}$$

417 which can be rewritten

$$418 \quad f_{\mu,l}^{\alpha,n+\frac{1}{2}} = f_{\mu,l}^{\alpha,n} - \Delta t \sum_{k=1}^3 \Phi_{k,l}(f_{\mu,l}^{\alpha,n}, f_{\mu_k,l}^{\alpha,n}, n_k),$$

419 where for $f, g \in \mathbb{R}^4$ and $n \in \mathbb{R}^2$,

$$420 \quad \Phi_{k,l,\mu}(f, g, n) = ((V_l \cdot n)^+ f - (V_l \cdot n)^- g) \frac{|\Gamma_k|}{|T_\mu|}.$$

421 **LEMMA 4.1.** *Let λ_1 and λ_2 be defined in (3.6). The upwind scheme (4.4) is*
 422 *monotone if and only if the following CFL condition holds:*

$$423 \quad (4.5) \quad \Delta t \max_{1 \leq d \leq 2} \frac{\lambda_d}{\Delta x_d} \leq \frac{1}{4}.$$

424 *Proof.* For a given triangle T_μ with edges Γ_k and outward unit normal vectors n_k
 425 we have to satisfy the condition

$$426 \quad \forall l \in \{1, 2, 3, 4\}, \quad \frac{\Delta t}{|T_\mu|} \sum_{k=1}^3 (V_l \cdot n_k)^+ |\Gamma_k| \leq 1.$$

427 It is necessary to compute the quantities $G = \frac{|\Gamma_k|}{|T_\mu|} V_l \cdot n_k$, for each type of interface.
 428 In the setting chosen here, there exist four types of edges:

- 429 • Vertical edges ($n = e_1$): $G = 4 \frac{v_{1,l}}{\Delta x_1}$.
- 430
- 431 • Horizontal edges ($n = e_2$): $G = 4 \frac{v_{2,l}}{\Delta x_2}$.
- 432
- 433 • Diagonal edges similar to the ones between subcells 1 and 2 on figure 1:
 434 $G = 2 \left(\frac{v_{1,l}}{\Delta x_1} - \frac{v_{2,l}}{\Delta x_2} \right)$.
- 435
- 436 • Diagonal edges similar to the ones between subcells 1 and 4 on figure 1:
 437 $G = 2 \left(\frac{v_{1,l}}{\Delta x_1} + \frac{v_{2,l}}{\Delta x_2} \right)$.

438 The result is then achieved straightforwardly. \square

439 The remaining steps for the subcell T_μ are the same as in the cartesian case, in
 440 particular the homogeneity property of remark 3.1 is still available. Macroscopic
 441 fluxes for species α can be defined as

$$442 \quad \forall (U, V) \in \mathbb{R}^4, \quad \mathcal{F}_{k,\mu}^\alpha(U, V, n_k) = \sum_{l=1}^4 \Phi_{k,l,\mu}(M_l^\alpha(U), M_l^\alpha(V), n_k)$$

443 and we obtain

$$\begin{cases}
 \rho_\mu^{n+1} = \rho_\mu^n - \Delta t \sum_{k=1}^3 \mathcal{F}_{k,\mu,1}^n, \\
 \rho_\mu^{n+1} u_\mu^{n+1} = \rho_\mu^n u_\mu^n - \Delta t \sum_{k=1}^3 \mathcal{F}_{k,\mu,2}^n, \\
 \mathcal{E}_\mu^{e,n+1} = \mathcal{E}_\mu^{e,n} - \Delta t \sum_{k=1}^3 \mathcal{F}_{k,\mu,3}^n + \Delta t u_\mu^{n+1} \cdot \sum_{k=1}^3 \delta_{k,\mu}^n + \Delta t \nu^{ei} (T_\mu^{i,n+1} - T_\mu^{e,n+1}), \\
 \mathcal{E}_\mu^{i,n+1} = \mathcal{E}_\mu^{i,n} - \Delta t \sum_{k=1}^3 \mathcal{F}_{k,\mu,4}^n - \Delta t u_\mu^{n+1} \cdot \sum_{k=1}^3 \delta_{k,\mu}^n - \Delta t \nu^{ei} (T_\mu^{i,n+1} - T_\mu^{e,n+1}),
 \end{cases}$$

444

445 where

$$\begin{aligned}
 \mathcal{F}_{k,\mu,1}^n &= \sum_{\alpha} \mathcal{F}_{k,\mu,1}^{\alpha}(U_{\mu}^{\alpha,n}, U_{\mu_k}^{\alpha,n}, n_k), & \mathcal{F}_{k,\mu,2}^n &= \sum_{\alpha} \mathcal{F}_{k,\mu,2}^{\alpha}(U_{\mu}^{\alpha,n}, U_{\mu_k}^{\alpha,n}, n_k), \\
 \mathcal{F}_{k,\mu,3}^n &= \mathcal{F}_{k,\mu,3}^e(U_{\mu}^{e,n}, U_{\mu_k}^{e,n}, n_k), & \mathcal{F}_{k,\mu,4}^n &= \mathcal{F}_{k,\mu,3}^i(U_{\mu}^{i,n}, U_{\mu_k}^{i,n}, n_k),
 \end{aligned}$$

446

447 and

$$\delta_{k,\mu}^n = -c^i \mathcal{F}_{k,\mu,2}^e(U_{\mu}^{e,n}, U_{\mu_k}^{e,n}, n_k) + c^e \mathcal{F}_{k,\mu,2}^i(U_{\mu}^{i,n}, U_{\mu_k}^{i,n}, n_k) \in \mathbb{R}^2.$$

448

449 Computation of partial energies is similar to the first-order scheme, by the resolution
 450 of 2×2 system.

451 Finally, denoting $\mathcal{U}_j^{(i),n+1}$ the value obtained in subcell number $T_j^{(i)}$, solution at
 452 time t^{n+1} is defined by:

$$\mathcal{U}_j^{n+1} = \frac{1}{4} \sum_{i=1}^4 \mathcal{U}_j^{(i),n+1}.$$

453

454 Again if $\gamma^e = \gamma^i$, the positivity of ρ and of the total temperature are preserved under
 455 appropriate reconstruction and CFL condition.

456 **5. Numerical results.** In this section, the second-order method developed pre-
 457 viously is validated by a series of test cases: 1D Riemann problem extended to 2D,
 458 2D Riemann problem with four states and an implosion test case.

459 For all test cases, the following physical parameters are fixed: Boltzmann constant
 460 $k_B = 1.3807 \times 10^{-23}$ J.K $^{-1}$, electronic particular mass $m^e = 9,1094 \times 10^{-31}$ kg, ionic
 461 particular mass $m^i = 1.6726 \times 10^{-27}$ kg and elementary electric charge $e = -q^e =$
 462 $q^i = 1.6022 \times 10^{-19}$ C. Ionization rate Z is fixed at 1.

463 The first problem we have to deal with is the choice of the velocities λ_d^{\pm} . As
 464 a matter of fact, due to the physical values involved: high temperatures, strong
 465 differences between electronic and ionic masses, the theoretical condition (2.26) largely
 466 overestimates the needed values. Hence the computed solutions are highly diffusive,
 467 even for refined grids. This is due to the fact that there is a high difference between
 468 the electronic and ionic sound velocities. Consequently we choose to use the global
 469 sound velocity:

$$(5.1) \quad \forall \mathcal{U} \in \Omega, \quad \frac{\lambda_d^-}{2} < u_d - a < u_d + a < \frac{\lambda_d^+}{2}, \quad d = 1, 2$$

470

471 where a is defined in (2.7).

472 **5.1. 1D to 2D.** The goal of our first test case is to establish the consistency of
 473 the 2D code with already obtained 1D results. In [8] and [13] the one-dimensional first
 474 order version of the scheme presented here is compared to other first order schemes.
 475 It is noticed that in the presence of shocks, that is when the nonconservative products
 476 $u \cdot \nabla(c_i p_e - c_e p_i)$ are not well defined, the values of ionic and electronic temperatures
 477 are sensitive to the choice of the discretisation method. In particular, the 1D first
 478 order version of the scheme presented here is in good agreement with the DVM and
 479 the kinetic relaxed method, with physically meaningful results. In the present work,
 480 we want to verify that the values of discontinuous temperatures remain the same when
 481 1D and 2D versions of the the scheme are applied, and also when we move from first
 482 to second order. The second order 1D scheme is constructed with the same ideas as
 483 the 2D one.

484 Let $(\bar{\rho}, \bar{\rho} \bar{u}, \bar{\mathcal{E}}_e, \bar{\mathcal{E}}_i) \in \mathbb{R}^4$ a solution of the 1D bitemperature Euler system. For
 485 $\omega = (\cos \theta, \sin \theta)$ fixed, we define for $(x, t) \in \mathbb{R}^2 \times \mathbb{R}$:

$$486 \quad \rho(x, t) = \bar{\rho}(x \cdot \omega, t), \quad u(x, t) = \bar{u}(x \cdot \omega, t) \omega, \quad \mathcal{E}_\alpha(x, t) = \bar{\mathcal{E}}_\alpha(x \cdot \omega, t), \quad \alpha = e, i.$$

487 This defines a solution of the 2D system (2.5).

488 All quantities are in SI units. In order to prove that γ_i and γ_e are allowed to be
 489 distinct we choose $\gamma_e = 5/3$, $\gamma_i = 7/5$. We set $\bar{\rho}(x, 0) = 1$, $\bar{u}(x, 0) = 0$, and electronic
 490 and ionic initial temperatures are:

$$491 \quad \begin{aligned} \bar{T}^e(x, 0) &= 2.3 \times 10^6 \quad \text{if } x < \frac{1}{2}, \quad \bar{T}^e(x, 0) = 2.3 \times 10^7 \quad \text{else,} \\ \bar{T}^i(x, 0) &= 1.7406 \times 10^6 \quad \text{if } x < \frac{1}{2}, \quad \bar{T}^i(x, 0) = 1.7406 \times 10^7 \quad \text{else.} \end{aligned}$$

492 The rotation angle is $\theta = -\pi/12$. Final simulation time is set equal to $t = 4.0901 \times$
 493 10^{-7} . In this test case, we set $\nu^{ei} = 4 \times 10^9$, so that the ionic and electronic tem-
 494 peratures remain distinct. The 1D test is performed on a 800 points uniform mesh of
 495 $[0, 1]$, while the 2D test is performed on a 800×800 uniform mesh of $[0, 1] \times [0, 1]$.

496 In figure 2 we present the total 2D density ρ (left) and electronic temperature
 497 (right) for the second order scheme. Then we compare 1D results with 2D values on
 498 a segment along the propagation direction $\omega = (\cos \theta, \sin \theta)$ passing by the center of
 499 the unit square. We focus on the electronic and ionic temperatures. The first order
 500 and second order 1D plateaux are identical, see figures 3 left (electronic) and right
 501 (ionic). The 1D and 2D results also coincide, see figures 4 left (electronic) and right
 502 (ionic).

503 **5.2. Four interfaces Riemann problem.** For this second test case, consider,
 504 on domain $[0, 1] \times [0, 1]$, a partition in four quadrants of identical size. A constant
 505 state is chosen as initial data on each quadrant. Initial velocity is equal to zero over
 506 the whole domain and initial densities are as follows:

$$507 \quad \begin{cases} \rho(x_1, x_2, 0) = 1 \text{ kg.m}^{-3}, & \text{if } x_1 < 0.5 \text{ and } x_2 < 0.5, \\ \rho(x_1, x_2, 0) = 0.125 \text{ kg.m}^{-3}, & \text{if } x_1 < 0.5 \text{ and } x_2 > 0.5, \\ \rho(x_1, x_2, 0) = 0.125 \text{ kg.m}^{-3}, & \text{if } x_1 > 0.5 \text{ and } x_2 < 0.5, \\ \rho(x_1, x_2, 0) = 1 \text{ kg.m}^{-3}, & \text{if } x_1 > 0.5 \text{ and } x_2 > 0.5, \end{cases}$$

508

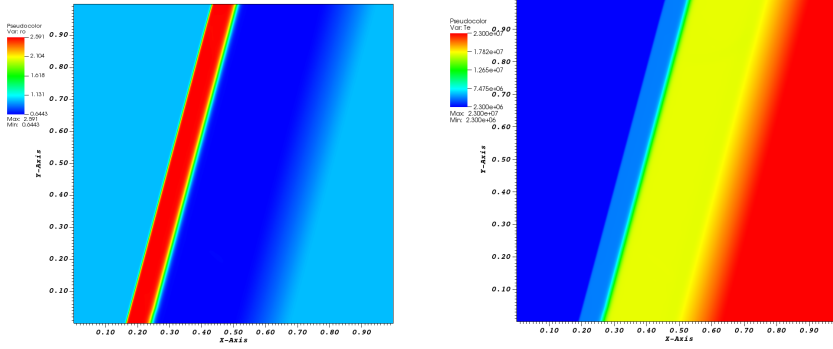


FIG. 2. Shock tube test case with $\nu^{ei} = 4 \times 10^9$, 800 by 800 points. Left: total density, right : electronic temperature.

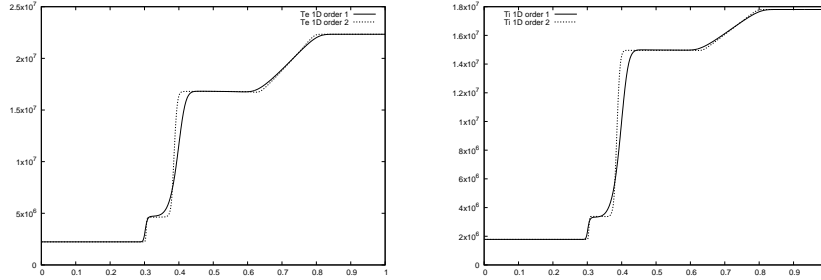


FIG. 3. Shock tube test case with $\nu^{ei} = 4 \times 10^9$, 800 by 800 points. 1D results. Left: electronic temperature, right: ionic temperature.

509 and initial electronic and ionic temperatures are defined by:

$$510 \quad \begin{cases} T^e(x_1, x_2, 0) = 293 \text{ K}, T^i(x_1, x_2, 0) = 273 \text{ K}, & \text{if } x_1 < 0.5 \text{ and } x_2 < 0.5, \\ T^e(x_1, x_2, 0) = 220 \text{ K}, T^i(x_1, x_2, 0) = 200 \text{ K}, & \text{if } x_1 < 0.5 \text{ and } x_2 > 0.5, \\ T^e(x_1, x_2, 0) = 220 \text{ K}, T^i(x_1, x_2, 0) = 200 \text{ K}, & \text{if } x_1 > 0.5 \text{ and } x_2 < 0.5, \\ 511 \quad T^e(x_1, x_2, 0) = 293 \text{ K}, T^i(x_1, x_2, 0) = 273 \text{ K}, & \text{if } x_1 > 0.5 \text{ and } x_2 > 0.5. \end{cases}$$

512 Here $\gamma^e = \gamma^i = 5/3$.

513 We compute the solution on a 2000×2000 grid. Final time is $t = 0.0001$. More-
514 over, we set $\nu^{ei} = 100 \text{ s}^{-1}$. Electronic temperature is presented in figure 5.

515 We proceed to cut the solution displayed on figure 5 along two different axis. The
516 first one is along axis $x_1 = 0.05$ and is displayed on figure 6 (left). The second one
517 is made along the axis $x_2 = 0.95$ and is visible on figure 6 (right). We retrieve the
518 solutions of the associate one-dimensional Riemann problems.

519 **5.3. Implosion test case.** In this test case, consider an implosion-type problem,
520 introduced in [20]. The physical domain is the square $[-1, 1] \times [-1, 1]$. We set $\gamma^e =$
521 $\gamma^i = 5/3$. Initial data for this Riemann problem is as follows: $\rho = 1 \text{ kg.m}^{-3}$, $u = 0$

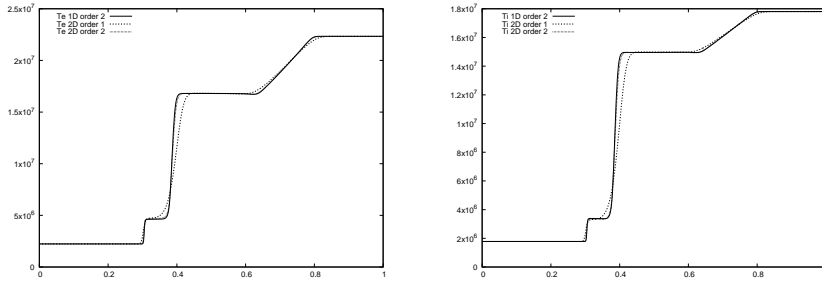


FIG. 4. Shock tube test case with $\nu^{ei} = 4 \times 10^9$, 800 by 800 points. 1D Vs 2D results along the propagation direction. Left: electronic temperature, right: ionic temperature.

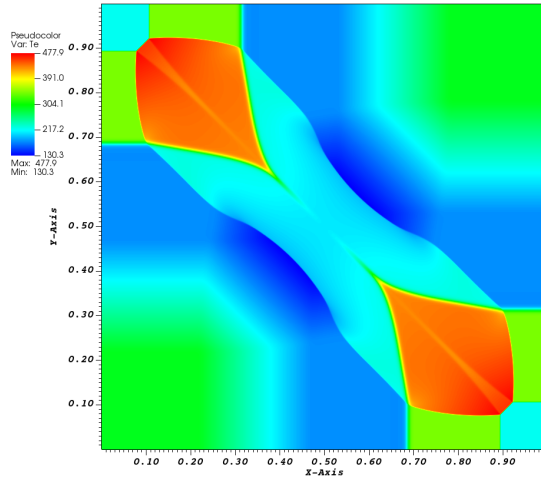


FIG. 5. Electronic temperature at time $t = 0.0001s$ for a four interfaces Riemann problem with $\nu^{ei} = 100 \text{ s}^{-1}$, with a grid of 2000 by 2000 points.

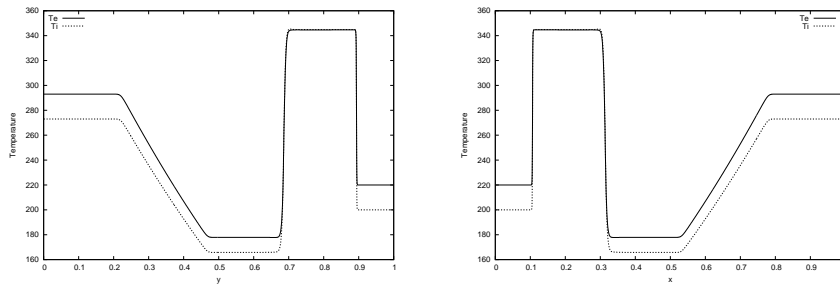


FIG. 6. Electronic and ionic temperatures at time $t = 0.0001s$ for a four interfaces Riemann problem with $\nu^{ei} = 100 \text{ s}^{-1}$, with a grid of 2000 by 2000 points along axis $x_1 = 0.05$ (left) and along axis $x_2 = 0.95$ (right).

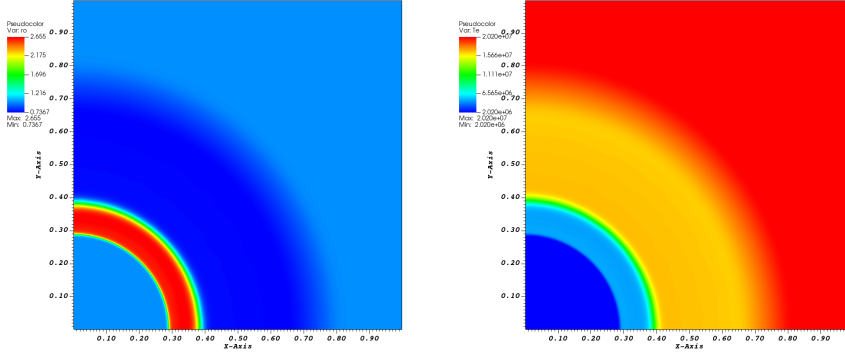


FIG. 7. Total density (left) and electronic temperature (right) at time $t = 4.0901 \times 10^{-7}$ s for a implosion test case with ν^{ei} given by the NRL formula with a grid of 500 by 500 points.

522 m.s⁻¹ and temperatures are given by:

$$\begin{aligned}
 523 \quad T^e(x_1, x_2, 0) &= 2,3 \times 10^6 K, \quad T^i(x_1, x_2, 0) = 1.7406 \times 10^6 K && \text{if } (x_1)^2 + (x_2)^2 < \frac{1}{4}, \\
 T^e(x_1, x_2, 0) &= 2,3 \times 10^7 K, \quad T^i(x_1, x_2, 0) = 1.7406 \times 10^7 K && \text{otherwise.}
 \end{aligned}$$

524 The relaxation frequency ν^{ei} is chosen realistically, according to the formulae given
 525 by the NRL formulary [21].

526 Thanks to symmetry properties of the problem, it is only necessary to solve it
 527 on the quarter domain $[0, 1] \times [0, 1]$, equipped with suitable boundary conditions. On
 528 figure 7, are given the isovalues of the total density and of the electronic temperature
 529 at time $t = 4.0901 \times 10^{-7}$ s.

530 We compare our results to the ones in [20], pages 48-52, which have been obtained
 531 by replacing the nonconservative bitemperature Euler system by a conservative one
 532 with the hypothesis that the electrons have an isentropic behaviour. Qualitatively, the
 533 results are similar, including the numerical values taken by densities, velocities and
 534 temperatures. The difference lies only on the velocity of propagation of the waves. In
 535 order to clarify this point we write the system in polar coordinates for such a solution:
 536 the velocity is a scalar function $v(r)$ multiplied by the radial vector $(\cos \theta, \sin \theta)$ so
 537 that $|u| = |v|$. One has

$$538 \quad \rho(x, t) = \bar{\rho}(r, t), \quad u(x, t) = v(r, t)(\cos \theta, \sin \theta), \quad \mathcal{E}^\alpha(x, t) = \bar{\mathcal{E}}^\alpha(r, t)$$

539 satisfying the following system:

$$540 \quad \begin{cases} \partial_t \bar{\rho} + \partial_r (\bar{\rho} v) = -\frac{1}{r} \bar{\rho} v \\ \partial_t (\bar{\rho} v) + \partial_r (\bar{\rho} v^2 + \bar{p}^e + \bar{p}^i) = -\frac{1}{r} \bar{\rho} v^2 \\ \partial_t \bar{\mathcal{E}}^e + \partial_r (v(\bar{\mathcal{E}}^e + \bar{p}^e)) + v \partial_r (c^e \bar{p}^i - c^i \bar{p}^e) = -\frac{1}{r} v (\bar{\mathcal{E}}^e + \bar{p}^e) + \nu_{ei} (\bar{T}^i - \bar{T}^e) \\ \partial_t \bar{\mathcal{E}}^i + \partial_r (v(\bar{\mathcal{E}}^i + \bar{p}^i)) - v \partial_r (c^e \bar{p}^i - c^i \bar{p}^e) = -\frac{1}{r} v (\bar{\mathcal{E}}^i + \bar{p}^i) + \nu_{ei} (\bar{T}^e - \bar{T}^i). \end{cases}$$

541 This one-dimensional system can be viewed as the 1D cartesian system with a source
 542 term, so we compute the solution by using a slight modification of the 1D cartesian

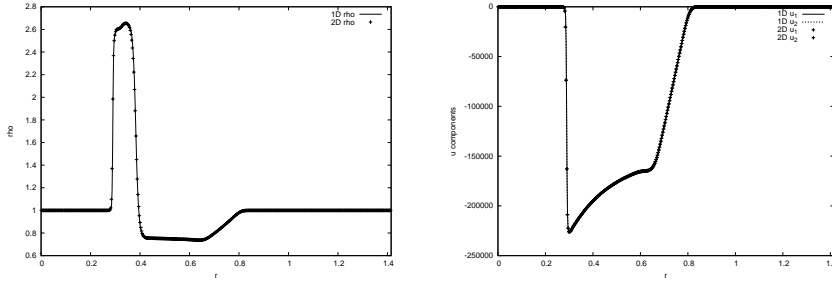


FIG. 8. Total density (left) and velocity (right) along the first bisector at time $t = 4.0901 \times 10^{-7} s$ for an implosion test case with v^{ei} given by the NRL formula with a grid of 500 by 500 points. Comparison with a 1D computation in polar coordinates.

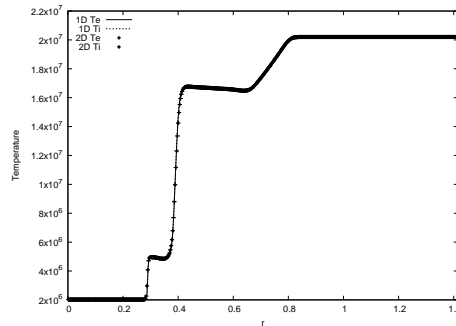


FIG. 9. Electronic and ionic temperatures along the first bisector at time $t = 4.0901 \times 10^{-7} s$ for an implosion test case with v^{ei} given by the NRL formula with a grid of 500 by 500 points. Comparison with a 1D computation in polar coordinates.

543 scheme. We find the same results as the 2D computation, as shown on figures 8, 9
 544 where a cut along the first bisector is provided: the total density and the components
 545 of the velocity are displayed on figure 8. On figure 9 on can observe that at final
 546 time, electronic and ionic temperatures have completely relaxed towards equilibrium
 547 : $T^i = T^e$. The discrepancy with the results of [20] can be due, either to the change
 548 of model, or, more probably to an error on the value of the final time of computation
 549 by those authors.

550 Finally we observe the peak of density at time $t = 8.798 \times 10^{-7} sec$, see figure 10.
 551

552 **6. Conclusion.** In this article, a BGK-type discrete velocity underlying kinetic
 553 system for the 2D bitemperature Euler system has been constructed in order to ap-
 554 proximate the bitemperature Euler system. It takes into account the force term
 555 induced by the electric field and it owns entropy dissipation properties that allow to
 556 prove that the numerical scheme is also entropy dissipative and therefore admissible
 557 in the sense defined in [8].

558 At first order and if $\gamma^e = \gamma^i$, we have shown that the total density, the velocity
 559 and the total energy provided by our scheme coincide with those provided by the HLL

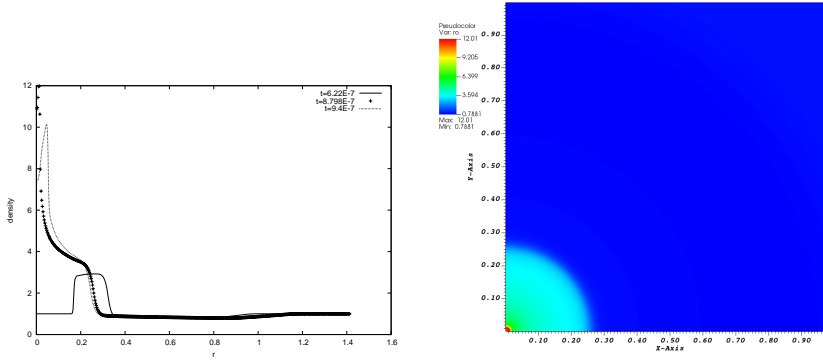


FIG. 10. Implosion test case with ν^{ei} given by the NRL formula with a grid of 500 by 500 points. Left: density along the first bisector at 3 different times: the peak occurs for $t = 8.798 \times 10^{-7}$ sec. Right: isovalues of the density when the peak occurs.

560 scheme. Consequently positivity of density and internal total energy are preserved un-
 561 der suitable conditions. The novelty lies in the approximation of the nonconservative
 562 terms *via* a discrete Ohm's law for the ionic and electronic energies.

563 Due to the special structure of the system, we had to develop a new procedure
 564 to obtain a second order extension of this scheme able to preserve the positivity
 565 properties, along with the conservation of the density, momentum and total energy.
 566 The Euler bitemperature system was introduced in the context of Inertial Confinement
 567 Fusion, where high densities and temperatures are involved. During this work we did
 568 not have problems of non positivity, so we did not investigate the effective way to
 569 preserve these properties. This will be done in a forthcoming work.

570 Several test cases have been performed in order to show the good behaviour of the
 571 method in different situations. We proved that the 2D results are in perfect agreement
 572 with the one-dimensional known ones, validated in [8]. Moreover, for the implosion
 573 test, we compared our results with the ones obtained in [20] with a simplified conser-
 574 vative model. A discrepancy appeared, which led us to perform 1D computations in
 575 polar coordinates which seem to confirm our results.

576 In order to go towards more realistic applications, we aim to integrate magnetic
 577 fields in the bitemperature Euler model. In [12], starting from a kinetic system coupled
 578 with the Maxwell system in the transverse magnetic configuration, we have derived
 579 a bitemperature system and developed a Suliciu relaxation scheme. Hence we shall
 580 address the discrete BGK model including magnetic fields in a forthcoming paper.

581

REFERENCES

- 582 [1] R. ABGRALL AND S. KARNI, *A comment on the computation of non-conservative products*,
 583 *Journal of Computational Physics*, 229 (2010), pp. 2759–2763.
 584 [2] D. AREGBA-DRIOLLET AND S. BRULL, *About viscous approximations of the bitemperature euler*
 585 *system*, *Communications in Math Sciences*, 17 (2019), pp. 1135–1147.
 586 [3] D. AREGBA-DRIOLLET AND S. BRULL, *Modelling and numerical study of the polyatomic bitem-*
 587 *perature euler system*. submitted, 2020.
 588 [4] D. AREGBA-DRIOLLET, S. BRULL, AND X. LHÉBRARD, *Nonconservative hyperbolic systems in*
 589 *fluid mechanics*, in SMAI 2017—8ème Biennale Française des Mathématiques Appliquées
 590 et Industrielles, vol. 64 of ESAIM Proc. Surveys, EDP Sci., 2018.
 591 [5] D. AREGBA-DRIOLLET AND R. NATALINI, *Discrete kinetic schemes for systems of conservation*

- 592 laws, in *Hyperbolic problems: theory, numerics, applications*, Vol. I (Zürich, 1998), vol. 129
 593 of *Internat. Ser. Numer. Math.*, Birkhäuser, Basel, 1999, pp. 1–10.
- 594 [6] D. AREGBA-DRIOLLET AND R. NATALINI, *Discrete kinetic schemes for multidimensional systems*
 595 *of conservation laws*, *SIAM Journal on Numerical Analysis*, 37 (2000), pp. 1973–2004.
- 596 [7] D. AREGBA-DRIOLLET, R. NATALINI, AND S. TANG, *Explicit diffusive kinetic schemes for non-*
 597 *linear degenerate parabolic systems*, *Math. Comp.*, 73 (2004), pp. 63–94.
- 598 [8] D. AREGBA-DRIOLLET, J. BREIL, S. BRULL, B. DUBROCA, AND E. ESTIBALS, *Modelling and nu-*
 599 *merical approximation for the nonconservative bitemperature Euler model*, *ESAIM: Math-*
 600 *ematical Modelling and Numerical Analysis*, 52 (2018), pp. 1353–1383.
- 601 [9] C. BERTHON, *Robustness of MUSCL schemes for 2D unstructured meshes*, *J. Comput. Phys.*,
 602 218 (2006), pp. 495–509.
- 603 [10] F. BOUCHUT, *Construction of BGK Models with a Family of Kinetic Entropies for a Given*
 604 *System of Conservation Laws*, *Journal of Statistical Physics*, 95 (1999), pp. 113–170.
- 605 [11] F. BOUCHUT, *Nonlinear stability of finite volume methods for hyperbolic conservation laws and*
 606 *well-balanced schemes for sources*, Birkhäuser Verlag, Basel, 2004.
- 607 [12] S. BRULL, B. DUBROCA, AND X. LHÉBRARD, *Modelling and entropy satisfying relaxation scheme*
 608 *for the nonconservative bitemperature euler system with transverse magnetic field*, *Com-*
 609 *puters and fluids*, 14 (2021).
- 610 [13] S. BRULL, B. DUBROCA, AND C. PRIGENT, *A kinetic approach of the bi-temperature euler model*,
 611 *Kinetic & Related Models*, 13 (2020), p. 33.
- 612 [14] C. CALGARO, E. CREUSÉ, T. GOUDON, AND Y. PENEL, *Positivity-preserving schemes for Euler*
 613 *equations: sharp and practical CFL conditions*, *J. Comput. Phys.*, 234 (2013), pp. 417–438.
- 614 [15] C. CHALONS AND F. COQUEL, *Navier-stokes equations with several independent pressurelaws*
 615 *and explicit predictor-corrector schemes*, *Numerische Math*, 103 (2005), pp. 451–478.
- 616 [16] G.-Q. CHEN, C. LEVERMORE, AND T.-P. LIU, *Hyperbolic conservation laws with stiff relaxation*
 617 *terms and entropy*, *Communications on Pure and Applied Mathematics*, 47 (1994), pp. 787–
 618 830.
- 619 [17] F. COQUEL AND C. MARMIGNON, *Numerical methods for weakly ionized gas*, *Astrophysics and*
 620 *Space Science*, 260 (1998), pp. 15–27.
- 621 [18] G. DAL MASO, P. LE FLOCH, AND F. MURAT, *Definition and weak stability of nonconservative*
 622 *products*, *Journal de mathématiques pures et appliquées*, 74 (1995), pp. 483–548.
- 623 [19] B. EINFELDT, C.-D. MUNZ, P. L. ROE, AND B. SJÖGREEN, *On Godunov-type methods near low*
 624 *densities*, *J. Comput. Phys.*, 92 (1991), pp. 273–295.
- 625 [20] E. ESTIBALS, H. GUILLARD, AND A. SANGAM, *Bi-temperature Euler Equations Modeling for*
 626 *Fusion Plasma*, Tech. Report RR-9026, INRIA Sophia-Antipolis, 2017.
- 627 [21] J. D. HUBA AND B. P. BRANCH, *2004 revised nrl plasma formulary*.
- 628 [22] T.-P. LIU, *Hyperbolic conservation laws with relaxation*, *Communications in Mathematical*
 629 *Physics*, 108 (1987), pp. 153–175.
- 630 [23] R. NATALINI, *A Discrete Kinetic Approximation of Entropy Solutions to Multidimensional*
 631 *Scalar Conservation Laws*, *Journal of Differential Equations*, 148 (1998), pp. 292–317.
- 632 [24] C. PARÉS, *Path-conservative numerical methods for nonconservative hyperbolic systems*, in
 633 *Numerical methods for balance laws*, vol. 24 of *Quad. Mat.*, Dept. Math., Seconda Univ.
 634 Napoli, Caserta, 2009, pp. 67–121.
- 635 [25] B. PERTHAME AND Y. QIU, *A variant of Van Leer’s method for multidimensional systems of*
 636 *conservation laws*, *J. Comput. Phys.*, 112 (1994), pp. 370–381.
- 637 [26] B. PERTHAME AND C.-W. SHU, *On positivity preserving finite volume schemes for Euler equa-*
 638 *tions*, *Numer. Math.*, 73 (1996), pp. 119–130.
- 639 [27] B. PERTHAME AND C.-W. SHU, *On positivity preserving finite volume schemes for Euler equa-*
 640 *tions*, *Numerische Mathematik*, 73 (1996), pp. 119–130.
- 641 [28] D. SERRE, *Relaxations semi-linéaire et cinétique des systèmes de lois de conservation*, *Ann.*
 642 *Inst. H. Poincaré Anal. Non Linéaire*, 17 (2000), pp. 169–192.
- 643 [29] E. TORO, *Riemann Solvers and Numerical Methods for Fluid Dynamics: A Practical Intro-*
 644 *duction*, Springer Berlin Heidelberg, 2009.
- 645 [30] Q. WARGNIER, S. FAURE, B. GRAILLE, T. MAGIN, AND M. MASSOT, *Numerical treatment of the*
 646 *nonconservative product in a multiscale fluid model for plasmas in thermal nonequilibrium:*
 647 *application to solar physics*, *SIAM. J. Sci. Comput.*, 42 (2020), pp. 1–27.